Journal of Applied Geophysics 111 (2014) 14–20

Contents lists available at ScienceDirect

Journal of Applied Geophysics

journal homepage: www.elsevier.com/locate/jappgeo

Frequency-wavenumber domain phase inversion along reflection wavepaths

Han Yu [a,*], Yunsong Huang [b,1]

[a] School of Computer Science & Technology, Nanjing University of Posts & Telecommunications, Nanjing 210046, China
[b] Division of Physical Sciences and Engineering, King Abdullah University of Science and Technology, Thuwal 23955-6900, Saudi Arabia

ARTICLE INFO

Article history:
Received 12 July 2014
Accepted 19 September 2014
Available online 28 September 2014

Keywords:
Phase inversion
Wavepaths
Frequency–wavenumber domain
Low-wavenumber

ABSTRACT

A background velocity model containing the correct low-wavenumber information is desired for both the quality of the migration image and the success of waveform inversion. To achieve this goal, the velocity is updated along the reflection wavepaths, rather than along both the reflection ellipses and transmission wavepaths as in conventional FWI. This method allows for reconstructing the low-wavenumber part of the background velocity model, even in the absence of long offsets and low-frequency component of the data. Moreover, in gradient-based iterative updates, instead of forming the data error conventionally, we propose to exploit the phase mismatch between the observed and the calculated data. The phase mismatch emphasizes a kinematic error and varies quasi-linearly with respect to the velocity error. The phase mismatch is computed (1) in the frequency–wavenumber (f–k) domain replacing the magnitudes of the calculated common shot gather by those of the observed one, and (2) in the temporal–spatial domain to form the difference between the transformed calculated common-shot gather and the observed one. The background velocity model inverted according to the proposed methods can serve as an improved initial velocity model for conventional waveform inversion. Tests with synthetic and field data show both the benefits and limitations of this method.

1. Introduction

Full waveform inversion (FWI) has attracted much research in both the space–time and space–frequency methods (Pratt et al., 1998; Tarantola, 1984, 1986). It has also been successfully applied to some data sets (Sheng et al., 2006; Shin and Min, 2006; Sirgue and Pratt, 2004), but its success largely depends on the accuracy of the initial velocity model. A small deviation of the initial velocity model may degrade the travel time information and consequently the migration image quality. Thus, obtaining a good background velocity model is a fundamental requirement for seismic inversion (Virieux and Operto, 2009).

Traveltime tomography methods (Aki and Richards, 2002; Pratt and Goulty, 1991; Zhu and McMechan, 1989) can provide a relatively reliable background velocity model for FWI that only inverts the early arrivals. The depth of the velocity model that traveltime tomography can invert for depends on the maximum source-to-receiver offset. Recently, Xu et al. (2012) proposed to boost the low-wavenumber component for updating the velocity model by singling out the reflection wavepaths, thereby enabling the inversion for deep parts of the model without long offset data. This method mainly focuses on inverting the background velocity (Qin et al., 2013; Wang et al., 2013), rather than generating a highly resolved tomogram. The velocity model is decoupled into one inverted from low-wavenumber transmission updates and the other from high-wavenumber reflection updates. These two components are alternatively updated during the iterations. At each iteration step, the image is firstly migrated from the data and then demigrated to obtain the difference between the observed and the demigrated data. This difference is then smeared back along the wavepaths for the gradient.

Previous methods for calculating the data residual use either direct subtraction (Tarantola, 1984) or cross correlation (Luo and Schuster, 1991) between the calculated and the observed data. In this work, we extend a method proposed by Sun and Schuster (1993) to mitigate the amplitude difference while retaining the phase difference between the calculated and the observed data sets. We will present the theory and workflow first, and then show the numerical results with both synthetic and field data. The final section is the conclusion.

1.1. Theory and workflow

Without loss of generality, we treat the subsurface velocity distribution $v(\mathbf{x})$ as the combination of a background velocity model $v_0(\mathbf{x})$ and a reflectivity model $\delta v(\mathbf{x})$ such that

$$v(\mathbf{x}) = v_0(\mathbf{x}) + \delta v(\mathbf{x}). \quad (1)$$

* Corresponding author. Tel.: +86 25 52620227.
E-mail addresses: nanking.yu@gmail.com, han.yu@njupt.edu.cn (H. Yu), yunsong.huang@kaust.edu.sa (Y. Huang).
[1] Tel.: +966 12 808 0290.

http://dx.doi.org/10.1016/j.jappgeo.2014.09.012
0926-9851/

To update $v_0(\mathbf{x})$ using the reflection wavepaths is to minimize the following waveform misfit function (Xu et al., 2012)

$$E = \tfrac{1}{2}\,||d_{obs}-d_{calc}||^2, \tag{2}$$

where d_{obs} denotes the observed data mostly consisting of the reflection energy, and d_{calc} denotes the demigrated data using the Born approximation. The derivative $\partial E/\partial v_0(\mathbf{x})$ of E with respect to v_0 by fixing the reflectivity model δv is utilized to compute the wavepaths for updating v_0 iteratively (Xu et al., 2012).

To construct the misfit gradient, we start from the acoustic wave equation in the space–time ($\mathbf{x}$–t) domain

$$\frac{1}{v_0^2(\mathrm{x})}\frac{\partial^2 p(\mathrm{x},t|\mathrm{x}_s)}{\partial^2 t}-\frac{\partial^2 p(\mathrm{x},t|\mathrm{x}_s)}{\partial^2 x}-\frac{\partial^2 p(\mathrm{x},t|\mathrm{x}_s)}{\partial^2 z}=f(\mathrm{x}_s,t), \tag{3}$$

where $p(\mathbf{x}, t|\mathbf{x}_s)$ denotes the pressure field trace recorded at the subsurface position $\mathbf{x}$, with listening time t and a source at $\mathbf{x}_s$ excited at $t = 0$ described by the function $f(\mathbf{x}_s,t)$. For simplicity, we will use the indices $\boldsymbol{s}$ and $\boldsymbol{r}$ to respectively represent the source position $\mathbf{x}_s$ and the receiver position $\mathbf{x}_r$. The first step of inversion is to migrate the observed data d_{obs} with the initial velocity model $v_0^{(1)}(\mathbf{x})$ to obtain the image $m(\mathbf{x})$. This migration image m is then used to generate the demigrated data d_{calc} with the Lippmann–Schwinger equation under the Born approximation. The data mismatch Δd between d_{obs} and d_{calc} is estimated to create the virtual sources for the backpropagation. To calculate the reflection wavepaths, the backpropagated wavefields are correlated with the forward wavefields at zero-lag. The overall gradient consists of two parts: one from the source to the image and the other from the image to the receiver (Fig. 1).

Based on this method, the background velocity model v_0 can be updated along the wavepaths from the shot locations to reflectors, and then back to the receiver positions. This workflow can be summarized in the frequency domain with six steps:

1. The observed data are first migrated to estimate the reflectivity model by

$$m(\mathbf{y}) = Re\left\{\Sigma_{s,r,\omega}\omega^2 D_{obs}(r|s)\left(W(\omega)G(\mathbf{y}|s)G(\mathbf{y}|r)\right)^*\right\}. \tag{4a}$$

   Here and hereafter, D_{obs} and D_{calc} represent d_{obs} and d_{calc} in the space–frequency domain. $W(\omega)$ is the source spectrum and ω denotes the angular frequency. $G(\mathbf{y}|\boldsymbol{s})$ is the Green's function of wave propagating from $\boldsymbol{s}$ to $\mathbf{y}$.
2. The source side upgoing wavefield is computed using the image $m(\mathbf{y})$ by

$$U_s(\mathbf{x}) = \Sigma_{\mathbf{y}}\omega^2 G(\mathbf{x}|\mathbf{y})m(\mathbf{y})W(\omega)G(\mathbf{y}|s). \tag{4b}$$

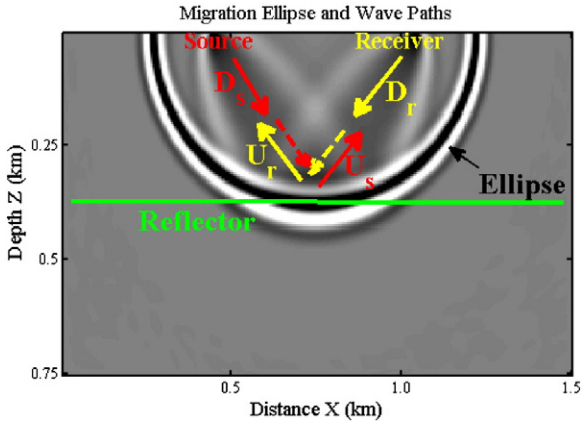

Fig. 1. The migration ellipse and reflection wavepaths (Yu et al., 2014a).

3. The receiver side downgoing or backpropagated wavefield recorded at $\mathbf{x}_r$ is constructed by backpropagating the data residual $\Delta D = D_{obs} - D_{calc}$ using

$$D_r(\mathbf{x}) = \Sigma_r \Delta D^*(r|s)G(\mathbf{x}|r). \tag{4c}$$

4. Similarly, the receiver side upgoing wavefield can be obtained by

$$U_r(\mathbf{x}) = \Sigma_{\mathbf{y},r} G(\mathbf{x}|\mathbf{y})m(\mathbf{y})\Delta D^*(r|s)G(\mathbf{y}|r). \tag{4d}$$

5. The source-side downgoing wavefield for the source at $\mathbf{x}_s$ is obtained by forward modeling with the low-wavenumber background velocity model using

$$D_s(\mathbf{x}) = \omega^2 W(\omega)G(\mathbf{x}|s). \tag{4e}$$

6. Finally, the background velocity model is updated by the gradient consisting of two pairs of upgoing and downgoing wavefields, namely the reflection wavepaths:

$$v_0^{(n+1)}(\mathbf{x}) = v_0^{(n)}(\mathbf{x}) - \alpha Re\left\{\Sigma_{\omega,s}\left(D_r U_s^* + D_s U_r^*\right)\right\}. \tag{4f}$$

In Eqs. (4a)–(4f), the upgoing and downgoing waves are respectively represented by U and D with subscripts r or s; $G(\mathbf{y}|\boldsymbol{s})$ is the Green's function for the source at $\boldsymbol{s}$ and the receiver at $\mathbf{y}$. With a very simple two layered velocity model, the reflection wavepaths can be clearly discerned in Fig. 1 and the migration ellipse is dropped in the inversion using Eq. (4f).

However, to calculate the step length α, it is still necessary to compare D_{obs} with D_{calc} in order to determine if the newly updated $v_0(\mathbf{x})$ is more accurate than from the previous iteration. Therefore, the migration and demigration procedures need to be revisited again. Errors between the finite difference data and the demigrated data (Woodward, 1989) suggest that a direct subtraction may not be a good strategy. Because the traveltime error, which varies quasi-linearly with velocity error, is related to the phase difference between the calculated and the observed data, to focus on the phase difference and to omit the amplitude difference, Sun and Schuster (1993) proposed to equate the amplitude spectra of two traces before taking their difference. Therefore the difference of the equalized traces is only sensitive to the phase mismatch. We extend the method of Sun and Schuster (1993) to the f–k domain as follows. For any source $\boldsymbol{s}$, both the recorded common shot gather (CSG) d_{obs} and the calculated CSG d_{calc} are 2D-Fourier transformed ( ) in the frequency–wavenumber (f–k) domain to obtain their magnitude spectrum and a phase spectrum θ,

$$\dot{D}_{obs}(r|s) = \mathcal{F}(d_{obs}(r,\ t|s)) = A_{obs}(r,\omega,k;s)\ \exp\left[i\theta_{obs}(r,\omega,k;s)\right], \tag{5a}$$

$$\dot{D}_{calc}(r|s) = \mathcal{F}(d_{calc}(r,t|s)) = A_{calc}(r,\omega,k;s)\ \exp\left[i\theta_{calc}(r,\omega,k;s)\right]. \tag{5b}$$

Here, $\dot{D}$ denotes the recorded data in the f–k domain rather than the space–frequency domain. The amplitude spectrum A_{calc} of the calculated CSG is replaced by the amplitude A_{obs} of the observed CSG, so there is only a phase mismatch in the residual. Unlike the method of Sun and Schuster (1993) that deals with each pair of traces individually (Yu et al., 2014a), the proposed method treats the entire CSG as a whole. (We call the former method 'trace-based' and the latter method 'CSG-based'.) Therefore, by keeping the original phase spectrum only, the transformed calculated data are obtained:

$$\underline{D}_{calc}(r|s) = A_{obs}exp(i\theta_{calc}). \tag{5c}$$

Consequently, the slopes of the transformed demigrated data closely approximate the correct ones. This fact is highlighted in Fig. 2, where